Journal of Computational Physics 395 (2019) 125–143

Contents lists available at ScienceDirect

Journal of Computational Physics

www.elsevier.com/locate/jcp

Multi-symplectic quasi-interpolation method for Hamiltonian partial differential equations

Zhengjie Sun [a,b,*]

[a] Department of Mathematics, Hong Kong Baptist University, Hong Kong
[b] Shanghai Key Laboratory for Contemporary Applied Mathematics, School of Mathematical Sciences, Fudan University, Shanghai, PR China

ARTICLE INFO

Article history:
Received 15 January 2019
Received in revised form 30 May 2019
Accepted 8 June 2019
Available online 12 June 2019

Keywords:
Multi-symplectic PDEs
Quasi-interpolation
Multi-symplectic conservation law
Energy conservation
Momentum conservation

ABSTRACT

In this paper, we propose a multi-symplectic quasi-interpolation method for solving multi-symplectic Hamiltonian partial differential equations. Based on the method of lines, we first discretize the multi-symplectic PDEs using quasi-interpolation method and then employ appropriate time integrators to obtain the full-discrete system. The local conservation properties including multi-symplectic conservation laws, energy conservation laws and momentum conservation laws are discussed in detail. For illustration, we provide two concrete examples: the nonlinear wave equation and the nonlinear Schrödinger equation. The salient feature of our multi-symplectic quasi-interpolation method is that it is valid both on uniform grids and nonuniform grids. The numerical results show the good accuracy and excellent conservation properties of the proposed method.

1. Introduction

It is widely recognized that the Hamiltonian partial differential equations (PDEs) have the symplectic structure which can help tracking the long time behavior of the system. Besides, the Hamiltonian PDEs also have a multi-symplectic formulation [3–5,12,28,29,31,35,39,41], which can be used to study the local property of the system. Since multi-symplecticity is a geometry feature of the multi-symplectic Hamiltonian PDEs, it is of great importance to preserve this property when performing the numerical simulations. A standard method for obtaining the multi-symplectic method is first to discretize the PDE in space and then integrate the semi-discrete system in time. Various approaches can be utilized in spatial discretization, such as the finite difference method [4], the finite element method [54], the Runge-Kutta collocation method [39], the spectral method [5,10], the wavelet collocation method [56,57] and so on.

However, the above mentioned methods are required to generate a suitable mesh, which is difficult for solving problems with complicated and irregular geometries. Thus it is necessary to develop a meshless multi-symplectic method that can deal with scattered data in complex domains. One choice of meshless methods is the quasi-interpolation. It has been found applications in many areas of computational mathematics[11,27,47,49,55]. It is very flexible and easy to implement without solving any linear system. It also has been shown to possess good accuracy and excellent stability when simulating high-order derivatives [33,34]. Hence, the purpose of this paper is to generalize the quasi-interpolation method to construct the multi-symplectic scheme for solving Hamiltonian PDEs on multi-symplectic formulation.

* Correspondence to: Department of Mathematics, Hong Kong Baptist University, Hong Kong.
E-mail address: sunzhengjie1218@163.com.

https://doi.org/10.1016/j.jcp.2019.06.026
0021-9991/

We consider the multi-symplectic Hamiltonian PDE of type

$$\mathbf{M}\partial_t \mathbf{z} + \mathbf{K}\partial_x \mathbf{z} = \nabla_{\mathbf{z}} S(\mathbf{z}),\ \mathbf{z} \in \mathbb{R}^m, (x,t) \in \mathbb{R}^2, \tag{1.1}$$

where $\mathbf{M}, \mathbf{K} \in \mathbb{R}^{m\times m}$ are two skew-symmetric matrices and $S : \mathbb{R}^m \to \mathbb{R}$ is a smooth function.

The multi-symplectic formulation attracts much attention for several reasons [3,35], one of the most important is the multi-symplectic conservation law

$$\partial_t \omega + \partial_x \kappa = 0, \tag{1.2}$$

where ω and κ are the pre-symplectic forms defined as follows

$$\omega = \frac{1}{2} d\mathbf{z} \wedge \mathbf{M} d\mathbf{z},\ \ \kappa = \frac{1}{2} d\mathbf{z} \wedge \mathbf{K} d\mathbf{z},$$

where $\wedge$ is the wedge product. Besides, the system has the following local energy conservation law

$$\partial_t E(\mathbf{z}) + \partial_x F(\mathbf{z}) = 0, \tag{1.3}$$

where E is the energy density and F is the energy flux

$$E(\mathbf{z}) = S(\mathbf{z}) - \frac{1}{2}\mathbf{z}^T \mathbf{K}\partial_x \mathbf{z}, \quad F(\mathbf{z}) = \frac{1}{2}\mathbf{z}^T \mathbf{K}\partial_t \mathbf{z}.$$

Moreover, the system also has a local momentum conservation law

$$\partial_t I(\mathbf{z}) + \partial_x G(\mathbf{z}) = 0, \tag{1.4}$$

with

$$I(\mathbf{z}) = \frac{1}{2}\mathbf{z}^T M\mathbf{z}_x, \quad G(\mathbf{z}) = S(\mathbf{z}) - \frac{1}{2}\mathbf{z}^T M\mathbf{z}_t.$$

A lot of famous PDEs can be written as the above multi-symplectic formulation, such as the Hamiltonian wave equation, the Schrödinger equation, the KdV equation, the shallow water equation, the Boussinesq equation (just name a few). For illustration, the wave equation and the Schrödinger equation are considered in this paper. Our multi-symplectic scheme is constructed through the method of lines with the quasi-interpolation method utilized in the spatial discretization and an appropriate time integrator used in temporal discretization. The main contributions of this paper go as follows:

- This is the first attempt to design multi-symplectic methods based on quasi-interpolation. From a kernel function satisfying the generalized Strang-Fix condition, we construct the generalized quasi-interpolation and use its derivatives to simulate the derivatives of the unknown function. Then employing the collocation method together with an appropriate time integrator to derive the final full-discrete system.
- The multi-symplectic quasi-interpolation method has $N + 1$ local multi-symplectic conservation laws, local energy conservation laws and local momentum laws. Moreover, our approach can easily deal with nonuniform grids, it is a meshless method.
- The numerical results demonstrate that our method is efficient, easy to implement and also has good accuracy. Besides, the conservation properties of new multi-symplectic method are also verified.

The rest of paper is organized as follows. In section 2, we propose the multi-symplectic quasi-interpolation method for solving general multi-symplectic PDEs and derive the corresponding local conservation laws. Section 3 and section 4 discuss the multi-symplectic quasi-interpolation scheme for the nonlinear wave equation and the one-dimensional nonlinear Schrödinger equation respectively. Section 5 employs the multi-symplectic quasi-interpolation method together with tensor-product technique for solving the two-dimensional Schrödinger equation. Section 6 presents several numerical examples to test the efficiency, accuracy and the conservation properties of our new multi-symplectic method. Finally, we conclude the paper in section 7.

2. Multi-symplectic quasi-interpolation method for multi-symplectic PDEs

In this section, we first introduce the general quasi-interpolation method and then use it to construct the new multi-symplectic scheme. Our multi-symplectic quasi-interpolation scheme consists of three steps: firstly, we construct a quasi-interpolation through the sampling data. Secondly, using such quasi-interpolation in the space discretization to obtain the semi-discrete system. Finally, we derive the full-discrete scheme by employing the implicit midpoint method.

2.1. Quasi-interpolation method

Quasi-interpolation method has become an important tool in approximation theory and its applications. Compared with interpolation method, it computes the approximation directly without need to solve any linear system. Thus, it is simple, efficient and easy to implement. (For more details, one can refer to [1,6–8,13,48] and references therein.)

A simple quasi-interpolation scheme was proposed by Schoenberg (also known as Schoenberg's model [38])

$$Qf(x) = \sum_{j\in\mathbb{Z}} f(jh)\psi\left(\frac{x}{h} - j\right). \tag{2.1}$$

It has been found applications in the representation of curves and surfaces and the reconstruction of band-limited functions. It is well known that the Schoenberg's model provides an approximation order k if and only if the kernel ψ satisfies the following Strang-Fix conditions [22].

Definition 2.1 *(Strang-Fix conditions of order k).* A kernel function satisfies the Strang-Fix conditions of order k if the following estimates hold,

$$\begin{cases} \hat{\psi}(t) = 1 + \mathcal{O}(t^k), & t \to 0, \\ \hat{\psi}(2j\pi + t) = \mathcal{O}(t^k), & t \to 0,\ j \in \mathbb{Z}. \end{cases}$$

There are many functions satisfying the Strang-Fix conditions such as the symmetric B-splines, the multiquadric kernels, the linear combinations of conditional positive definite functions and so on. However, there are also a lot of functions don't satisfy the full Strang-Fix condition but only satisfy the first part of the Strang-Fix condition. In such circumstances, we can still construct the quasi-interpolation scheme which was developed by Wu and Liu [48]

$$Qf(x) = c_h \sum_{j\in\mathbb{Z}} f(jh)\psi\left(c_h\left(\frac{x}{h} - j\right)\right),\ x \in \mathbb{R}. \tag{2.2}$$

Now the approximation order of above quasi-interpolant is not k but still dependent on k by choosing the parameter $c_h = c(h)$ properly. In scheme (2.2), the kernel satisfies only the first part of Strang-Fix conditions

$$\hat{\psi}(t) = 1 + \mathcal{O}(t^k),\ t \to 0,$$

we call it the generalized Strang-Fix condition of order k.

The quasi-interpolation scheme (2.2) also has a counterpart in scattered data case, namely

$$Qf(x) = \sum_j f(x_j)\psi_\epsilon\left(x - x_j\right)\Delta_j, \quad \psi_\epsilon(x) = \frac{1}{\epsilon}\psi\left(\frac{x}{\epsilon}\right), \tag{2.3}$$

where $\int_{\mathbb{R}} \psi(x)dx = 1$ and Δ_j are some weights of quadrature. Here we first discuss the univariate case of the quasi-interpolation and then generalize it to the multivariate case by using tensor-product technique.

From the reference [48], we have the following theorem about the error estimate of scheme (2.3).

Theorem 2.1. *Let the kernel $\psi \in C^\mu(\mathbb{R})$ and has an algebraic decay $|\psi| \le o(1+|x|)^{-s-1}$ and satisfies $\int \psi(x)dx = 1$, $\hat{\psi} \in C^s$. Assume further that $f \in C^\gamma(\mathbb{R})$ with $\mu \ge \gamma$ and its Fourier transform $\hat{f}(t) \le o(1+|t|)^{-1-\gamma}$. Suppose the quadrature weights $\{\Delta_j\}$ possess an approximation order γ, then let $\epsilon = \mathcal{O}(h^{\frac{s+\gamma}{2s+\gamma}})$, we have*

$$\left|\sum_j f(x_j)\psi_\epsilon(x - x_j)\Delta_j - f(x)\right| \le \mathcal{O}(h^{\frac{s\gamma}{2s+\gamma}}).$$

According to the classical approximation theory, we have the following theorem about the approximation order of derivatives.

Theorem 2.2. *Under the assumptions of Theorem 2.1 and the condition $\frac{s\gamma}{2s+\gamma} > k$, the following estimate holds*

$$\left|\sum_j f(x_j)\psi_\epsilon^{(k)}(x - x_j)\Delta_j - f^{(k)}(x)\right| \le \mathcal{O}(h^{\frac{s\gamma}{2s+\gamma}-k}).$$

In the following sections, we shall use the quasi-interpolation scheme (2.3) to construct our new multi-symplectic method. In order to simplify the notation, we use ψ to replace ψ_ϵ in the sequels.

2.2. Space discretization

In this section, we discretize the multi-symplectic PDEs (1.1) in space by using quasi-interpolation method. Assume that $\mathbf{z} = (z_1(x,t), \ldots, z_m(x,t))^T$, the space collocation points are $X = \{x_j\}_{j=0}^N$ which could be uniform or nonuniform, then for each z_l, we construct the quasi-interpolation

$$z_l^*(x,t) = Q z_l(x,t) = \sum_{j=0}^{N} z_l(x_j,t)\psi(x-x_j)\Delta_j, l = 1, \ldots, m. \tag{2.4}$$

After that, the approximation of first derivative at data points can be derived from this quasi-interpolant

$$(Q z_l)'(x_k,t) = \sum_{j=0}^{N} z_l(x_j,t)\psi'(x_k-x_j)\Delta_j \approx z_l'(x_k,t). \tag{2.5}$$

Denoting $\mathbf{z}_k = \mathbf{z}|_{x=x_k} = (z_1(x_k,t), \ldots, z_m(x_k,t))^T$, we solve the equation (1.1) at collocation points and obtain

$$\mathbf{M}\frac{d}{dt}\mathbf{z}_k + \mathbf{K}(Q\mathbf{z})'|_{x=x_k} = \nabla_{\mathbf{z}} S(\mathbf{z}_k),\ k = 0, 1, \ldots, N, \tag{2.6}$$

where $Q\mathbf{z} = (Qz_1, \ldots, Qz_m)^T$. Substituting each Qz_l by (2.4) leads to

$$\mathbf{M}\frac{d}{dt}\mathbf{z}_k + \mathbf{K}\left(\sum_{j=0}^{N}\psi'(x_k-x_j)\Delta_j\mathbf{z}_j\right) = \nabla_{\mathbf{z}} S(\mathbf{z}_k), k = 0, 1, \ldots, N. \tag{2.7}$$

Before verifying the conservation properties of our algorithm, we give a property of the quasi-interpolation kernel in the following proposition.

Proposition 2.1. *Assume that the kernel $\psi(x) \in C^1(\mathbb{R})$ is given by the form $\psi(x) = f(x^2/2)$ (here f is called the f-form of $\psi(x)$ [40]) and suppose further that $X = \{x_j\}_{j=0}^N$ are the distinct collocation points, then the matrix $\Psi_1 = (\psi'(x_j - x_k))$ is skew-symmetric.*

Proof. Differentiating the kernel $\psi(x)$, we obtain $\psi'(x) = xf'(x^2/2)$. Thus $\psi'(x_j - x_j) = 0$ and

$$\psi'(x_j-x_k) = (x_j-x_k)f'((x_j-x_k)^2/2) = -(x_k-x_j)f'((x_k-x_j)^2/2) = -\psi'(x_k-x_j),$$

which completes the proof. □

Remark 2.1. In Proposition 2.1, we use the f-form of the kernel function $\psi(x)$. It is well-known that commonly used kernels can be written into that form [25,40], such as the multiquadric function ($\psi(x) = \sqrt{c^2+x^2}$), the Gauss function ($\psi(x) = e^{-(cx)^2/2}$), the inverse multiquadric function of order $2k$ ($\psi(x) = (c^2+x^2)^{-\frac{2k-1}{2}}$), polyharmonic kernels ($\psi(x) = |x|^{2k+1}$) and so on.

The system (2.7) has $N+1$ semi-discrete multi-symplectic conservation laws and local energy conservation laws.

Theorem 2.3. *The semi-discrete system (2.7) has the following $N+1$ multi-symplectic conservation laws*

$$\frac{d}{dt}\omega_k + \sum_{j=0}^{N}\psi'(x_k-x_j)\Delta_j\kappa_{kj} = 0,\ k = 0, 1, \ldots, N, \tag{2.8}$$

where $\omega_k = \frac{1}{2}(d\mathbf{z}_k \wedge \mathbf{M}d\mathbf{z}_k)$, $\kappa_{kj} = d\mathbf{z}_k \wedge \mathbf{K}d\mathbf{z}_j$. In addition, the total symplecticity is also preserved

$$\frac{d}{dt}\omega = 0,\ \omega = \sum_{k=0}^{N}\omega_k\Delta_k. \tag{2.9}$$

Proof. The variational equation of (2.7) is

$$\mathbf{M}\frac{d}{dt}d\mathbf{z}_k + \mathbf{K}\left(\sum_{j=0}^{N}\psi'(x_k-x_j)\Delta_j d\mathbf{z}_j\right) = S_{\mathbf{zz}}(\mathbf{z}_k)d\mathbf{z}_k, k = 0, 1, \ldots, N. \tag{2.10}$$

Taking the wedge product of both sides of (2.10) with $d\mathbf{z}_k$ gives

$$\frac{1}{2}\frac{d}{dt}(d\mathbf{z}_k \wedge \mathbf{M}d\mathbf{z}_k) + d\mathbf{z}_k \wedge \mathbf{K}\left(\sum_{j=0}^{N}\psi'(x_k - x_j)\Delta_j d\mathbf{z}_j\right) = 0,\ k = 0, 1, \ldots, N, \tag{2.11}$$

due to the fact that

$$\mathbf{z}_j \wedge \mathbf{M}\mathbf{z}_k = \mathbf{z}_k \wedge \mathbf{M}\mathbf{z}_j,\ \ d\mathbf{z}_k \wedge S_{\mathbf{zz}}(\mathbf{z}_k)d\mathbf{z}_k = 0.$$

Thus we obtain $N+1$ multi-symplectic conservation laws.

In addition, we can sum (2.8) over the spatial index and obtain

$$\frac{d}{dt}\sum_{k=0}^{N}\omega_k\Delta_k + \sum_{k=0}^{N}\sum_{j=0}^{N}\Delta_k\psi'(x_k - x_j)\Delta_j\kappa_{kj} = 0.$$

Noting that $(\psi'(x_k - x_j))$ is skew symmetric and $\kappa_{kj} = \kappa_{jk}$, we have

$$\frac{d}{dt}\sum_{k=0}^{N}\omega_k\Delta_k = 0.$$

It implies that the total symplecticy is preserved. □

Remark 2.2. In the proof of Theorem 2.3, we actually require that the matrix $\Delta\Phi_1\Delta$ is skew-symmetric, which can be ensured by Proposition 2.1 whether for uniform or nonuniform grids. In addition, we define the total symplecticity as $\omega = \sum_{k=1}^{N}\omega_k\Delta_k$ because the total symplecticity in Hamiltonian equations is an integral ([39,49,58]) and $\omega = \sum_{k=1}^{N}\omega_k\Delta_k$ is regard as the discretization of that integral.

Theorem 2.4. *The semi-discrete system (2.7) has $N+1$ local energy conservation laws*

$$\frac{d}{dt}E_k + \sum_{j=0}^{N}\psi'(x_k - x_j)\Delta_j F_{kj} = 0,\ \ k = 0, 1, \ldots, N, \tag{2.12}$$

where

$$E_k = S(\mathbf{z}_k) - \frac{1}{2}\sum_{j=0}^{N}\psi'(x_k - x_j)\Delta_j\langle\mathbf{z}_k, \boldsymbol{K}\mathbf{z}_j\rangle, \quad F_{kj} = \frac{1}{2}\left[\langle\mathbf{z}_k, \boldsymbol{K}(\mathbf{z}_j)_t\rangle + \langle\mathbf{z}_j, \boldsymbol{K}(\mathbf{z}_k)_t\rangle\right].$$

Here $\langle\cdot,\cdot\rangle$ means the inner product.

Proof. Taking the inner product of (2.7) with $(\mathbf{z}_k)_t$ and noting that $\mathbf{M}^T = -\mathbf{M}$, we have

$$\langle\mathbf{M}(\mathbf{z}_k)_t, (\mathbf{z}_k)_t\rangle = 0 \quad \text{and} \quad \langle\nabla_{\mathbf{z}}S(\mathbf{z}_k), (\mathbf{z}_k)_t\rangle = \frac{d}{dt}S(\mathbf{z}_k),$$

thus

$$\langle\mathbf{K}\sum_{j=0}^{N}\psi'(x_k - x_j)\Delta_j\mathbf{z}_j, (\mathbf{z}_k)_t\rangle = \frac{d}{dt}S(\mathbf{z}_k). \tag{2.13}$$

By a simple calculation, we obtain that

$$\begin{aligned}
&\langle\mathbf{K}\sum_{j=0}^{N}\psi'(x_k - x_j)\Delta_j\mathbf{z}_j, (\mathbf{z}_k)_t\rangle \\
&= \sum_{j=0}^{N}\psi'(x_k - x_j)\Delta_j\langle\mathbf{K}\mathbf{z}_j, (\mathbf{z}_k)_t\rangle \\
&= \frac{1}{2}\frac{d}{dt}\sum_{j=0}^{N}\psi'(x_k - x_j)\Delta_j\langle\mathbf{K}\mathbf{z}_j, \mathbf{z}_k\rangle - \frac{1}{2}\sum_{j=0}^{N}\psi'(x_k - x_j)\Delta_j\left[\langle\mathbf{K}(\mathbf{z}_j)_t, \mathbf{z}_k\rangle + \langle\mathbf{K}(\mathbf{z}_k)_t, \mathbf{z}_j\rangle\right].
\end{aligned}$$

Therefore, the $N+1$ local energy conservation laws hold. □

2.3. Time discretization

The next step for obtaining multi-symplectic scheme is the time discretization. We integrate the semi-discrete system (2.7) with the implicit midpoint method and obtain the full-discrete multi-symplectic scheme

$$\mathbf{M}\frac{\mathbf{z}_k^{n+1}-\mathbf{z}_k^n}{\tau}+\mathbf{K}\left(\sum_{j=0}^{N}\psi'(x_k-x_j)\Delta_j\mathbf{z}_j^{n+1/2}\right)=\nabla_{\mathbf{z}}S(\mathbf{z}_k^{n+1/2}),k=0,1,\ldots,N, \tag{2.14}$$

where $\mathbf{z}_k^{n+1/2}=\frac{\mathbf{z}_k^{n+1}+\mathbf{z}_k^n}{2}$.

We can easily verify that the system (2.14) has the following full-discrete multi-symplectic conservation laws and the local energy and momentum conservation laws by adopting the technique from references [5,10,39,56,57].

Theorem 2.5. *The system (2.14) has $N+1$ full-discrete multi-symplectic conservation laws*

$$\frac{\omega_k^{n+1}-\omega_k^n}{\tau}+\sum_{j=0}^{N}\psi'(x_k-x_j)\Delta_j\kappa_{kj}^{n+1/2}=0,\ k=0,1,\ldots,N, \tag{2.15}$$

where

$$\omega_k^n=\frac{1}{2}(d\boldsymbol{z}_k^n\wedge\boldsymbol{M}d\boldsymbol{z}_k^n),\quad \kappa_{kj}^{n+1/2}=d\boldsymbol{z}_k^{n+1/2}\wedge\boldsymbol{K}d\boldsymbol{z}_j^{n+1/2}.$$

Proof. We firstly obtain the variational equation of system (2.14)

$$\mathbf{M}\frac{d\mathbf{z}_k^{n+1}-d\mathbf{z}_k^n}{\tau}+\mathbf{K}\left(\sum_{j=0}^{N}\psi'(x_k-x_j)\Delta_j d\mathbf{z}_j^{n+1/2}\right)=S_{\mathbf{zz}}(\mathbf{z}_k^{n+1/2})d\mathbf{z}_k^{n+1/2}. \tag{2.16}$$

Then taking the wedge product of both sides of equation (2.16) with $d\mathbf{z}_k^{n+1/2}$, we have

$$\left(\mathbf{M}\frac{d\mathbf{z}_k^{n+1}-d\mathbf{z}_k^n}{\tau}\right)\wedge\left(\frac{d\mathbf{z}_k^{n+1}+d\mathbf{z}_k^n}{2}\right)+\sum_{j=0}^{N}\psi'(x_k-x_j)\Delta_j\kappa_{kj}^{n+1/2}=0. \tag{2.17}$$

Finally, using the fact that

$$\mathbf{M}d\mathbf{z}_k^{n+1}\wedge d\mathbf{z}_k^n=d\mathbf{z}_k^{n+1}\wedge(\mathbf{M}^T d\mathbf{z}_k^n)=-d\mathbf{z}_k^{n+1}\wedge(\mathbf{M}d\mathbf{z}_k^n)=\mathbf{M}d\mathbf{z}_k^n\wedge d\mathbf{z}_k^{n+1},$$

we can easily derive the equation (2.15). □

Theorem 2.6. *The system (2.14) has $N+1$ local energy conservation laws*

$$\frac{E_k^{n+1}-E_k^n}{\tau}+\sum_{j=0}^{N}\psi'(x_k-x_j)\Delta_j F_{kj}^{n+1/2}=RE_k,\quad k=0,\ldots,N, \tag{2.18}$$

where

$$E_k^n=S(\boldsymbol{z}_k^n)-\frac{1}{2}\sum_{j=0}^{N}\psi'(x_k-x_j)\Delta_j\langle z_k^n,\boldsymbol{K}\boldsymbol{z}_j^n\rangle,$$

$$F_{kj}^{n+1/2}=\frac{1}{2}\left[\left\langle\boldsymbol{z}_k^{n+1/2},\boldsymbol{K}\frac{\boldsymbol{z}_j^{n+1}-\boldsymbol{z}_j^n}{\tau}\right\rangle+\left\langle\boldsymbol{z}_j^{n+1/2},\boldsymbol{K}\frac{\boldsymbol{z}_k^{n+1}-\boldsymbol{z}_k^n}{\tau}\right\rangle\right],$$

and local momentum conservation laws

$$\frac{I_k^{n+1}-I_k^n}{\tau}+\sum_{j=0}^{N}\psi'(x_k-x_j)\Delta_j G_{kj}^{n+1/2}=RM_k,\quad k=0,\ldots,N, \tag{2.19}$$

where

$$I_k^n = \frac{1}{2}\sum_{j=0}^{N}\psi'(x_k - x_j)\Delta_j\langle z_k^n, \boldsymbol{M}\boldsymbol{z}_j^n\rangle,$$

$$G_{kj}^{n+1/2} = S(\boldsymbol{z}_j^{n+1/2}) - \frac{1}{2}\left[\left\langle \boldsymbol{z}_k^{n+1/2}, \boldsymbol{M}\frac{\boldsymbol{z}_j^{n+1}-\boldsymbol{z}_j^n}{\tau}\right\rangle + \left\langle \boldsymbol{z}_j^{n+1/2}, \boldsymbol{M}\frac{\boldsymbol{z}_k^{n+1}-\boldsymbol{z}_k^n}{\tau}\right\rangle\right].$$

RE and RM are the residuals.

Proof. We omit the proof here since it is standard and can be founded in many references such as [5,10,39,56,57]. □

Remark 2.3. Here, we employ a second order implicit symplectic method in the temporal discretization for simplicity. One can also use other symplectic methods, such as composition methods, high-order Runge-Kutta methods and so on. From Frutos [14] and Reich [39], we see that the full-discrete system can not conserve both the multi-symplecticity and the energy except for the linear equations.

Up to now, we have obtained the multi-symplectic quasi-interpolation method (MSQIM) for the general multi-symplectic PDEs. In order to make the MSQIM be more applicable, we shall illustrate it through three concrete examples, the nonlinear wave equation, the one-dimensional Schrödinger equation and the two-dimensional Schrödinger equation.

3. Multi-symplectic quasi-interpolation method for the nonlinear wave equation

3.1. Multi-symplectic quasi-interpolation scheme

Consider the nonlinear wave equation

$$u_{tt} - u_{xx} + G'(u) = 0,\ u = u(x,t),\ (x,t) \in \mathbb{R}^2, \tag{3.1}$$

where $G : \mathbb{R} \to \mathbb{R}$. It is a class of nonlinear wave equation describing vibration and wave propagation phenomena. It also plays an important role in quantum mechanics. There are many numerical methods for the nonlinear wave equations, such as the finite difference method [23,39], the Fourier pseudo-spectral method [30], the wavelet collocation method [58], discontinuous Galerkin methods [32,45,51,53], radial basis function methods [15,17,20,21,49], etc. Here, we shall discuss the multi-symplectic quasi-interpolation method for the nonlinear wave equation.

By introducing canonical momenta $v = u_t$, $w = u_x$ and defining the state variable $\mathbf{z} = (u, v, w)^T$, the above system can be transformed into the following multi-symplectic structure

$$\mathbf{M}\mathbf{z}_t + \mathbf{K}\mathbf{z}_x = \nabla_{\mathbf{z}} S(\mathbf{z}), \tag{3.2}$$

where

$$\mathbf{M} = \begin{pmatrix} 0 & -1 & 0 \\ 1 & 0 & 0 \\ 0 & 0 & 0 \end{pmatrix},\quad \mathbf{K} = \begin{pmatrix} 0 & 0 & 1 \\ 0 & 0 & 0 \\ -1 & 0 & 0 \end{pmatrix}$$

and the Hamiltonian

$$S(\mathbf{z}) = \frac{1}{2}(v^2 - w^2) + G(u).$$

The corresponding multi-symplectic conservation law and energy conservation law are

$$\partial_t(du \wedge dv) - \partial_x(du \wedge dw) = 0 \tag{3.3}$$

and

$$\partial_t\left[\frac{1}{2}(w^2 + v^2) + G(u)\right] + \partial_x(-vw) = 0, \tag{3.4}$$

respectively.

Applying quasi-interpolation method for spatial discretization of the system (3.2) and implicit midpoint method for time discretization, we obtain the full-discrete scheme

$$\begin{cases} \frac{U^{n+1}-U^n}{\tau} = V^{n+1/2}, \\ \frac{V^{n+1}-V^n}{\tau} = \Psi_1 \Delta W^{n+1/2} - G'(U^{n+1/2}), \\ \Psi_1 \Delta U^{n+1/2} = W^{n+1/2}. \end{cases} \tag{3.5}$$

Here $U^n = (u_0^n, \ldots, u_N^n)^T$, $V^n = (v_0^n, \ldots, v_N^n)^T$, $W^n = (w_0^n, \ldots, w_N^n)^T$, $W^{n+1/2} = \frac{1}{2}(W^n + W^{n+1})$, $\Psi_1 = (\psi'(x_k - x_j))$, $\Delta = \mathrm{diag}(\Delta_j)$.

System (3.5) has an equivalent form

$$\frac{U^{n+1} - 2U^n + U^{n-1}}{\tau^2} = (\Psi_1\Delta)^2 \frac{U^{n+1} + 2U^n + U^{n-1}}{4} - \frac{1}{2}(G'(U^{n+1/2}) + G'(U^{n-1/2})). \tag{3.6}$$

The above equation is an implicit nonlinear scheme, we can use an iteration method to solve it, such as the Newton method and fixed-point iteration method.

3.2. Convergence analysis

In this section, we shall prove that the multi-symplectic quasi-interpolation scheme for the Hamiltonian wave equation (3.5) is convergent. First, we estimate the spatial approximation error of the quasi-interpolant. For the nonlinear wave equation, we are required to prove that $(\Psi_1\Delta)^2 f$ is an approximation to the second order derivatives of f.

Theorem 3.1. *Suppose that $f \in C^\gamma(\mathbb{R})$. Let the kernel ψ (which is the ψ_ϵ in Theorem 2.1) satisfies the assumptions of Theorem 2.1 with $\frac{s\gamma}{2s+\gamma} > 2$. Then we have the following error estimate*

$$\|Q_2 f - f''\|_\infty \le \mathcal{O}(h^{\frac{s\gamma}{2s+\gamma}-2}),$$

where $Q_2 := \Psi'(x)\Delta\Psi_1\Delta$, $\Psi'(x) = (\psi'(x - x_0), \ldots, \psi'(x - x_N))$.

Proof. We split the error into

$$\|Q_2 f - f''\|_\infty \le \|Q_2 f - (Qf)''\|_\infty + \|(Qf)'' - f''\|_\infty. \tag{3.7}$$

For the rightmost term, the classical approximation theory gives rise to

$$\|(Qf)'' - f''\|_\infty \le \mathcal{O}(h^{\frac{s\gamma}{2s+\gamma}-2}). \tag{3.8}$$

For the other term in (3.7), according to Theorem 2.2 and the boundness of kernel, we have

$$\begin{aligned}
\|Q_2 f - (Qf)''\|_\infty &= \|\Psi'(x)\Delta\left(\Psi'(x)\Delta f - f'(x)\right)|_X - \left(\Psi'(x)\Delta f - f'(x)\right)'\|_\infty + \|\Psi'(x)\Delta f'|_X - f''(x)\|_\infty \\
&\le Ch^{-1}\|\Psi(x)\Delta g|_X - g(x)\|_\infty + Ch^{-1}\left\|\Psi(x)\Delta f'|_X - f'(x)\right\|_\infty \\
&\le Ch^{-1}\|g\|_\infty + \mathcal{O}(h^{\frac{s\gamma}{2s+\gamma}-2}) \\
&\le Ch^{-1}\mathcal{O}(h^{\frac{s\gamma}{2s+\gamma}-1}) + \mathcal{O}(h^{\frac{s\gamma}{2s+\gamma}-2}) \\
&\le \mathcal{O}(h^{\frac{s\gamma}{2s+\gamma}-2}),
\end{aligned} \tag{3.9}$$

where $g = \Psi'(x)\Delta f - f'(x)$ and $g|_X = (g(x_0), \ldots, g(x_N))^T$.

Combining (3.8) and (3.9) completes the proof. □

Remark 3.1. Actually, the derivatives approximation order in above theorem is coarse and can be improved in some circumstances. In [33], the authors established that the k-th derivative approximation order of the multiquadric quasi-interpolation is $\mathcal{O}(h^{\frac{2}{k+1}})$ provided that the shape parameter is taken as $c_h = \mathcal{O}(h^{\frac{1}{k+1}})$. It implies that the multiquadric quasi-interpolation can approximate high-order derivatives ($k \ge 2$) though the approximation order to primitive function is only two. The similar property was observed in multiquadric trigonometric B-spline quasi-interpolation [24].

Now that we have established the spatial accuracy. The temporal convergence result is guaranteed by the implicit midpoint method and appears in a large amount of literature [9,26,36,50,58].

4. Multi-symplectic quasi-interpolation method for the one-dimensional Schrödinger equation

The nonlinear Schrödinger equation is the most important equation in quantum mechanics, describing a wide range of physical phenomenon, such as nonlinear optics, plasma physics, self-focusing in laser pulses and so on. There are many numerical methods for solving Schrödinger equations in the literature [10,16,18,19,26,41,42,52,56,57]. In this paper, we consider the cubic nonlinear Schrödinger equation

$$i\eta_t + \eta_{xx} + \alpha|\eta|^2\eta = 0 \tag{4.1}$$

with the periodic boundary condition. Here $\eta = \eta(x,t)$ is a complex function and $\alpha > 0$ is a real constant.

Let $\eta = u(x,t) + iv(x,t)$, the above equation can be transformed into

$$\begin{cases} u_t = -v_{xx} - \alpha(u^2+v^2)v, \\ v_t = u_{xx} + \alpha(u^2+v^2)u. \end{cases} \tag{4.2}$$

The multi-symplectic formulation is followed by introducing a pair of conjugate momentum $p = u_x$, $q = v_x$

$$\begin{cases} v_t - p_x = \alpha(u^2+v^2)u, \\ -u_t - q_x = \alpha(u^2+v^2)v, \\ u_x = p, \\ v_x = q, \end{cases} \tag{4.3}$$

with the Hamiltonian defined as

$$S = \frac{1}{2}\left(p^2 + q^2 + \frac{\alpha}{2}(u^2+v^2)^2\right).$$

Thus the system (4.3) is a special form of equation (1.1) with $z = (u, v, p, q)^T$ and

$$\mathbf{M} = \begin{pmatrix} 0 & -1 & 0 & 0 \\ 1 & 0 & 0 & 0 \\ 0 & 0 & 0 & 0 \\ 0 & 0 & 0 & 0 \end{pmatrix}, \quad \mathbf{K} = \begin{pmatrix} 0 & 0 & -1 & 0 \\ 0 & 0 & 0 & -1 \\ 1 & 0 & 0 & 0 \\ 0 & 1 & 0 & 0 \end{pmatrix}$$

The system has the multi-symplectic conservation law

$$\frac{\partial}{\partial t}(-du \wedge dv) + \frac{\partial}{\partial x}(-du \wedge dp - dv \wedge dq) = 0, \tag{4.4}$$

the energy and momentum conservation law

$$\frac{\partial}{\partial t}\left[\frac{1}{2}\left(\frac{\alpha}{2}(u^2+v^2)^2 - p^2 - q^2\right)\right] + \frac{\partial}{\partial x}(pu_t + qv_t) = 0, \tag{4.5}$$

and

$$\frac{\partial}{\partial t}(uq - vp) + \frac{\partial}{\partial x}\left[\frac{1}{2}\left(\frac{\alpha}{2}(u^2+v^2)^2 + p^2 + q^2 - uv_t + vu_t\right)\right] = 0. \tag{4.6}$$

By imposing appropriate boundary conditions, such as periodic boundary conditions, we can obtain the global energy conservation law

$$\frac{d}{dt}\mathcal{E}(t) = 0, \quad \mathcal{E}(t) := \frac{1}{2}\int_a^b \left(\frac{\alpha}{2}(u^2+v^2)^2 - p^2 - q^2\right)dx \tag{4.7}$$

and global momentum conservation law

$$\frac{d}{dt}\mathcal{M}(t) = 0, \quad \mathcal{M}(t) := \int_a^b (uq - vp)dx. \tag{4.8}$$

Applying quasi-interpolation method and implicit midpoint method to the multi-symplectic formulation of the NLS (4.3), we have

$$\begin{cases} \frac{V^{n+1}-V^n}{\tau} - (\Psi_1\Delta)P^{n+1/2} - \alpha\left((U^{n+1/2})^2 + (V^{n+1/2})^2\right)U^{n+1/2} = 0, \\ \frac{U^{n+1}-U^n}{\tau} + (\Psi_1\Delta)Q^{n+1/2} + \alpha\left((U^{n+1/2})^2 + (V^{n+1/2})^2\right)V^{n+1/2} = 0, \\ \Psi_1\Delta U^{n+1/2} = P^{n+1/2}, \\ \Psi_1\Delta V^{n+1/2} = Q^{n+1/2}. \end{cases} \tag{4.9}$$

Here $U^n = (u_0^n, \ldots, u_N^n)^T$, τ is the time step, $U^{n+1/2} = \frac{U^n+U^{n+1}}{2}$, and $\left[(U^{n+1/2})^2 + (V^{n+1/2})^2\right]U^{n+1/2} = [\ldots, ((u_j^{n+1/2})^2 + (v_j^{n+1/2})^2)u_j^{n+1/2}, \ldots]^T$.

By eliminating the vectors $P^{n+1/2}$ and $Q^{n+1/2}$, we obtain an equivalent full-discrete scheme

$$\begin{cases} U^{n+1} = U^n - \tau\left[(\Psi_1\Delta)^2 V^{n+1/2} + \alpha\left((U^{n+1/2})^2 + (V^{n+1/2})^2\right)V^{n+1/2}\right], \\ V^{n+1} = V^n + \tau\left[(\Psi_1\Delta)^2 U^{n+1/2} + \alpha\left((U^{n+1/2})^2 + (V^{n+1/2})^2\right)U^{n+1/2}\right]. \end{cases} \tag{4.10}$$

5. Multi-symplectic quasi-interpolation method for two-dimensional PDEs

To obtain multi-symplectic scheme for two-dimensional PDEs, we could use the developed quasi-interpolation method together with the tensor-product technique in spatial discretization and the symplectic scheme in time integration. In the following, for example, we give the multi-symplectic quasi-interpolation scheme of the two-dimensional Schrödinger equation, the other multi-symplectic Hamiltonian equations can be obtained in the same way. Consider the equation

$$\begin{cases} u_t = -v_{xx} - v_{yy} - \alpha(u^2+v^2)v, \\ v_t = u_{xx} + u_{yy} + \alpha(u^2+v^2)u, \end{cases} \tag{5.1}$$

and the corresponding multi-symplectic formulation

$$\begin{cases} v_t - (p_1)_x - (p_2)_y = \alpha(u^2+v^2)u, \\ -u_t - (q_1)_x - (q_2)_y = \alpha(u^2+v^2)v, \\ u_x = p_1, \quad u_y = p_2 \\ v_x = q_1, \quad v_y = q_2, \end{cases} \tag{5.2}$$

we apply the tensor-product quasi-interpolation method for spatial discretization and the implicit midpoint rule for time discretization and obtain

$$\begin{cases} \frac{V^{n+1}-V^n}{\tau} - A_1 P_1^{n+1/2} - A_2 P_2^{n+1/2} - \alpha\left((U^{n+1/2})^2 + (V^{n+1/2})^2\right) U^{n+1/2} = 0, \\ \frac{U^{n+1}-U^n}{\tau} + A_1 Q_1^{n+1/2} + A_2 Q_2^{n+1/2} + \alpha\left((U^{n+1/2})^2 + (V^{n+1/2})^2\right) V^{n+1/2} = 0, \\ A_1 U^{n+1/2} = P_1^{n+1/2}, \quad A_2 U^{n+1/2} = P_2^{n+1/2} \\ A_1 V^{n+1/2} = Q_1^{n+1/2}, \quad A_2 V^{n+1/2} = Q_2^{n+1/2}, \end{cases} \tag{5.3}$$

where $A_1 = (\Psi_1\Delta)\otimes I_{N+1}$, $A_2 = I_{N+1}\otimes(\Psi_1\Delta)$ and I_{N+1} is the $(N+1)\times(N+1)$ identity matrix. Here Ψ_1 is the quasi-interpolation differentiation matrix and is skew-symmetric (see Proposition 2.1).

Eliminating the variables $P_1^{n+1/2}$, $P_2^{n+1/2}$, $Q_1^{n+1/2}$, $Q_2^{n+1/2}$, the scheme (5.3) is equivalent to

$$\begin{cases} U^{n+1} = U^n - \tau\left[D_2 V^{n+1/2} + \alpha\left((U^{n+1/2})^2 + (V^{n+1/2})^2\right) V^{n+1/2}\right], \\ V^{n+1} = V^n + \tau\left[D_2 U^{n+1/2} + \alpha\left((U^{n+1/2})^2 + (V^{n+1/2})^2\right) U^{n+1/2}\right], \end{cases} \tag{5.4}$$

where $D_2 = (\Psi_1\Delta)^2\otimes I_{N+1} + I_{N+1}\otimes(\Psi_1\Delta)^2$.

6. Numerical examples

6.1. Nonlinear wave equation

Example 1. Let $G(u) = 1-\cos u$, we get the Sine-Gordon equation

$$u_{tt} - u_{xx} + \sin u = 0. \tag{6.1}$$

We consider the so-called breather solution on the form [2,43]

$$u(x,t) = 4\arctan\left(\vartheta^{-1}\sin(\vartheta\zeta t)\operatorname{sech}(\zeta x)\right), \quad \zeta = \frac{1}{\sqrt{1+\vartheta^2}}, \tag{6.2}$$

which gives rise to the following initial conditions,

$$u(x,0) = 0, \quad v(x,0) = u_t(x,0) = 4\zeta\operatorname{sech}(\zeta x).$$

In (6.2), ϑ represents the velocity of the soliton. On an infinite domain, the breather solution oscillates up and down with period $\frac{2\pi}{\vartheta\zeta}$. In this experiment, we take $\vartheta = 0.5$ and consider the periodic condition $u(-20,t) = u(20,t)$.

Firstly, we test the accuracy of our MSQI method. We solve the Sine-Gordon equation (6.1) till time $t=1$ with small time step $\tau = 0.001$. In the space discretization, we use the quasi-interpolation with multiquadric kernel $\psi(x) = \frac{c^2}{(c^2+x^2)^{3/2}}$, where c is the shape parameter. The corresponding RMS-error, Max-error, the posteriori convergence rates and CPU time are presented in Table 1. The RMS-error and max-error are defined as

$$\text{RMS-error} := \sqrt{\frac{1}{N+1}\sum_{j=0}^{N}(u(x_j,t_n)-\hat{u}(x_j,t_n))^2}, \quad \text{Max-error} := \max_{0\le j\le N}\left|u(x_j,t^n)-\hat{u}(x_j,t^n)\right|,$$

where $u(x_j,t^n)$ and $\hat{u}(x_j,t^n)$ are the accurate solution and numerical solution at (x_j,t^n) separately.

Table 1
Numerical results of MSQI for the Sine-Gordon equation with uniform grids, $c = 0.4h^{1/3}$.

N	RMS-error	rate	Max-error	rate	CPU(s)
200	4.7484e-4		2.8822e-3		0.20
400	1.9574e-4	1.279	1.1450e-3	1.332	0.38
800	7.9743e-5	1.295	4.5834e-4	1.321	1.60
1600	3.2211e-5	1.308	1.8363e-4	1.320	7.19

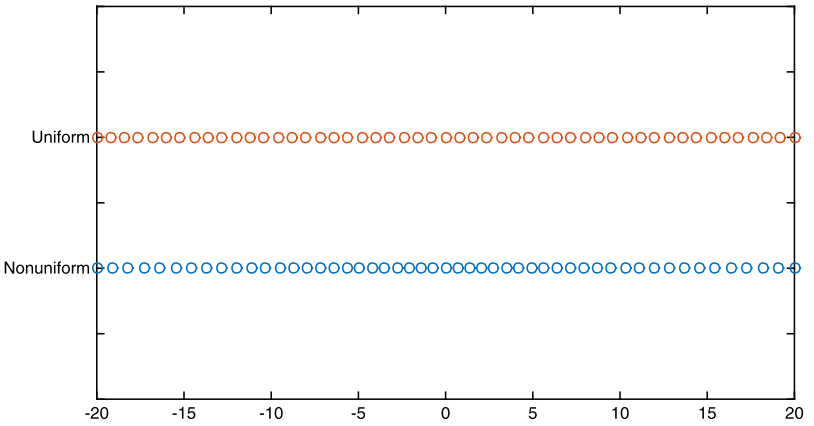

Fig. 1. Grids used for the numerical examples ($N = 50$).

Table 2
Numerical results of MSQI for the Sine-Gordon equation with nonuniform grids, $c = 0.4h^{1/3}$.

N	RMS-error	rate	Max-error	rate	CPU(s)
200	5.1667e-4		2.8636e-3		0.30
400	2.1456e-4	1.268	1.1438e-3	1.324	0.60
800	8.8301e-5	1.281	4.6217e-4	1.307	2.01
1600	3.6201e-5	1.286	1.8682e-4	1.307	9.78

Since our MSQI scheme is valid on nonuniform points, we solve the same problem on the following sampling centers [37]

$$\hat{x}_j = x_j - 0.9 \cdot \sin\left(\frac{\pi x_j}{L}\right), \quad x_j = -L + \frac{2jL}{N},\ L = 20,\ j = 0, \ldots, N.$$

Fig. 1 gives a comparison of uniform points and nonuniform points when $N = 50$. From the figure, we can see that the nonuniform points are more concentrated at the origin than the two sides. We solve the equation (6.3) using such nonuniform points with different grid numbers N and present the results in Table 2.

Then we solve the problem till $t = 100$ with time step $\tau = 0.01$ to investigate the long time behavior of our MSQI method. The global errors in the conserved quantities including the energy and the momentum can be found in Fig. 2 using both uniform and nonuniform centers. From this figure, we observe that whether for uniform or nonuniform cases, the energy and momentum are approximately conserved. Moreover, the approximated momentum on uniform girds achieves machine accuracy, which means that the momentum is preserved well with respect to time.

We also plot the errors in the local conservation laws to observe the variations of the residuals, which are given in Fig. 3 for uniform centers and 4 for nonuniform centers. It can be observed from these two figures that the errors are mainly concentrated around the origin.

6.2. One-dimensional nonlinear Schrödinger equation

Example 2 *(Single soliton).* Consider the NLS equation with one soliton equation

$$\eta(x,t) = \operatorname{sech}(x - 4t)e^{2i(\xi x - \frac{3}{2}t)}. \tag{6.3}$$

For accuracy test, we solve the problem in the domain $[-20, 20]$ till time $t = 1$ with $\xi = 1$. We use the full-discrete scheme (4.10) with the Gaussian kernels satisfying the generalized Strang-Fix condition of orders four and six respectively,

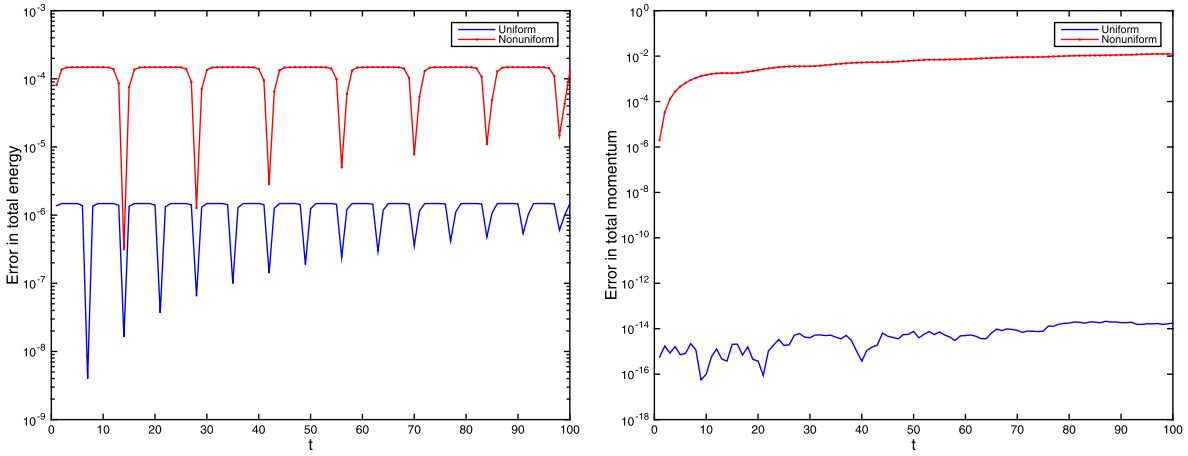

(a) Error in total energy (b) Error in total momentum

Fig. 2. Numerical errors in global energy and momentum over the time interval $[0, 100]$, Example 1.

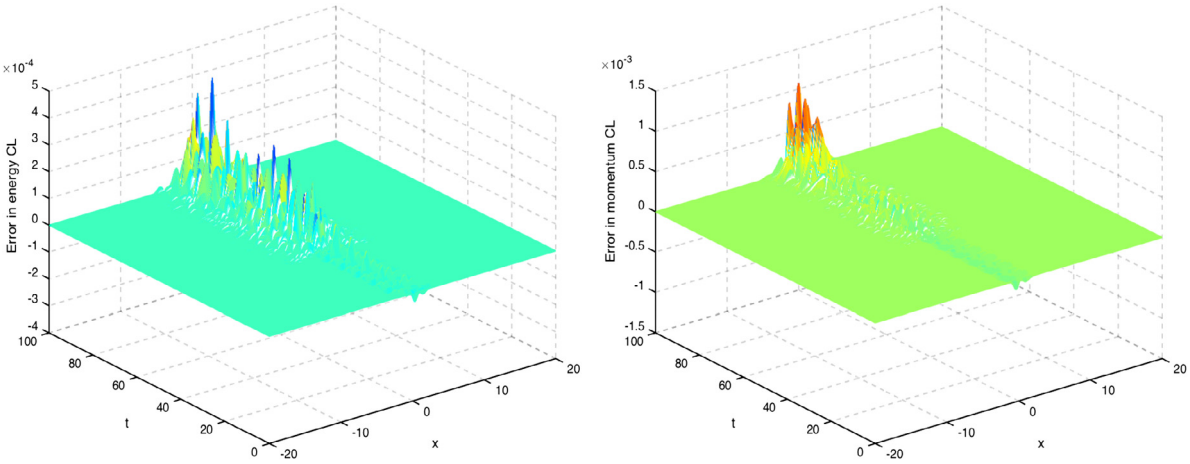

(a) Error in energy CL, uniform points (b) Error in momentum CL, uniform points

Fig. 3. Numerical errors in local energy and momentum over the time interval $[0, 100]$ on uniform points, Example 1.

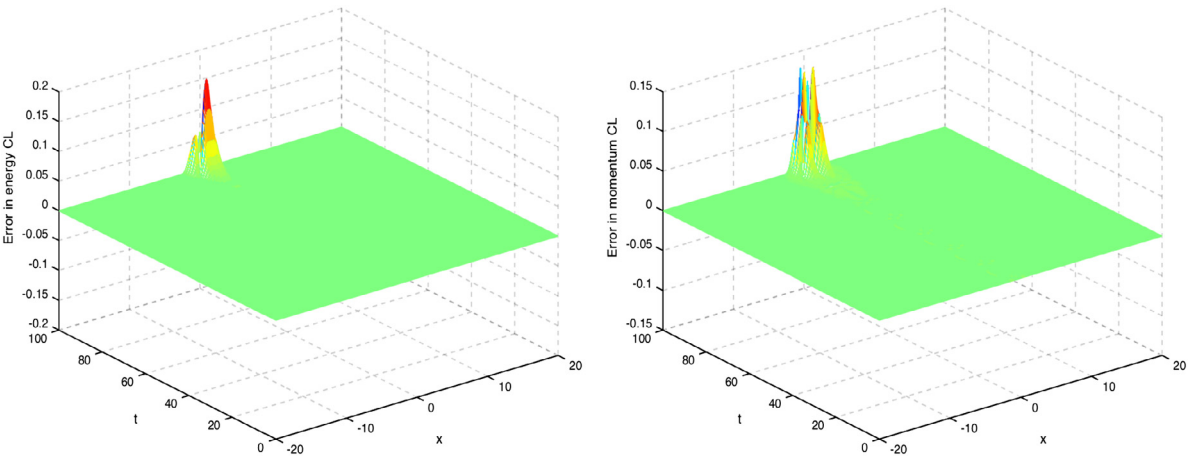

(a) Error in energy CL, nonuniform points (b) Error in momentum CL, nonuniform points

Fig. 4. Numerical errors in local energy and momentum over the time interval $[0, 100]$ on nonuniform points, Example 1.

Table 3
Numerical results of MSQI for the NLS equation with Gaussian kernel $\phi_1(x)$ (order four), the real part.

N	RMS-error	rate	Max-error	rate	CPU(s)
200	1.8609e-2		1.1741e-1		0.52
400	4.4189e-3	2.074	2.5917e-2	2.180	1.09
800	1.1186e-3	1.982	6.5622e-2	1.982	11.16
1600	2.8198e-4	1.988	1.6504e-3	1.991	85.81

Table 4
Numerical results of MSQI for the NLS equation with Gaussian kernel $\phi_2(x)$ (order six), the real part.

N	RMS-error	rate	Max-error	rate	CPU(s)
200	4.1110e-3		2.4490e-2		0.53
400	5.5269e-4	2.895	3.3646e-3	2.864	1.36
800	7.2549e-5	2.929	4.4170e-4	2.929	11.28
1600	8.2134e-6	3.143	4.9548e-5	3.156	87.69

Table 5
Numerical results of the finite difference method for the NLS equation, the real part.

N	RMS-error	rate	Max-error	rate	CPU(s)
200	8.8210e-2		4.8892e-1		0.39
400	2.2567e-2	1.967	1.3355e-1	1.872	0.63
800	5.5556e-3	2.022	3.2421e-2	2.042	10.52
1600	1.3820e-3	2.007	8.0414e-3	2.011	85.70

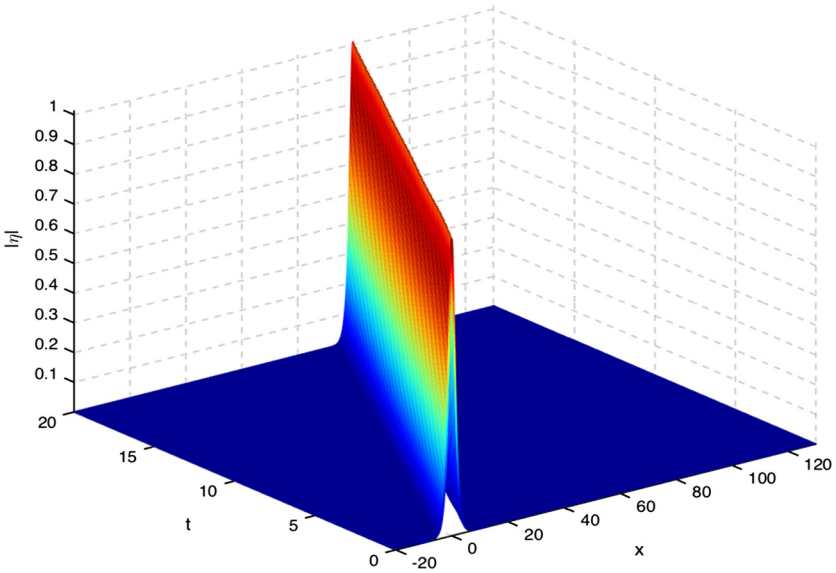

Fig. 5. The wave propagation of (6.3) by using MSQI scheme ($\tau = 0.001$, $N = 3200$), Example 2.

namely $\phi_1(x) = \frac{3c^2-x^2}{2\sqrt{2\pi}c^3} e^{-\frac{x^2}{2c^2}}$ and $\phi_2(x) = \frac{15c^4-10c^2x^2+x^4}{8\sqrt{2\pi}c^5} e^{-\frac{x^2}{2c^2}}$, where c is the shape parameter (for more details about such kernels, we refer the readers to [25]). The kernels satisfy high order generalized Strang-Fix condition and thus possesses high order convergence. To compute the nonlinear equation in (4.10), a fixed-point iteration method with tolerance 10^{-15} is adopted.

Table 3 and Table 4 give the RMS-error, the Max-error, the convergence rates and the CPU time for the real part of the solution with two different Gaussian kernels (the imaginary part has the similar phenomenon). Here the shape parameters are taken as $c = 0.4h^{1/2}$, $c = 0.5h^{1/2}$ respectively. Table 3 and Table 4 demonstrate that our MSQI method with Gaussian kernel $\phi_1(x)$ has about second order accuracy, while with Gaussian kernel $\phi_2(x)$ has about third order accuracy.

Moreover, for comparison, we also present the numerical results by using the second order finite difference method in Table 5. From Tables 3 and 5, we can observe that the CPU time by using our MSQI method and the finite difference method are almost the same, but our method provides more accurate solution.

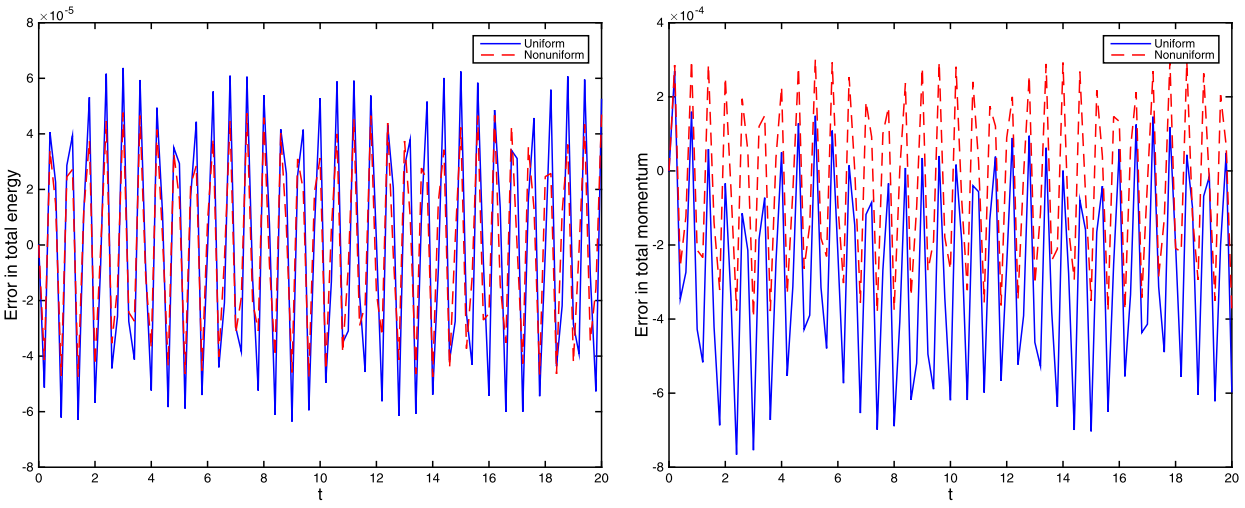

(a) Error in total energy (b) Error in total momentum

Fig. 6. Numerical errors in global energy and momentum over the time interval [0, 20], Example 2.

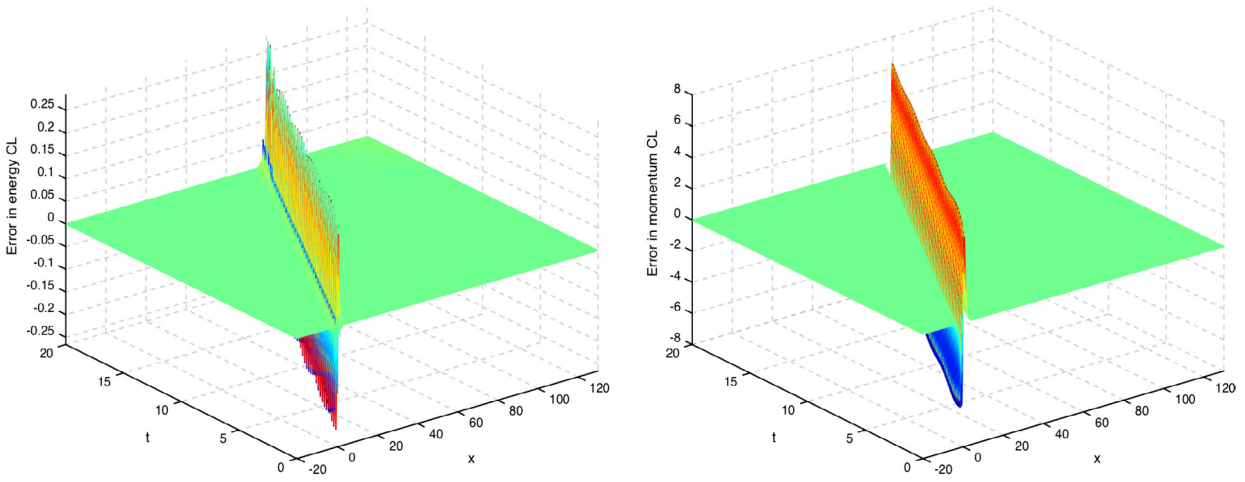

(a) Error in energy CL, uniform points (b) Error in momentum CL, uniform points

Fig. 7. Numerical errors in local energy and momentum over the time interval [0, 20] on uniform points, Example 2.

For long time simulations, we solve the equation till time $t = 20$ on the domain $[-20, 130]$ by using our MSQI method with the time step $\tau = 0.001$ and the grid number $N = 3200$. The Fig. 5 pictures the propagation of the approximated wave, which simulates the motion of exact soliton very well. The Fig. 6 shows the numerical errors in the conserved quantities including the total energy and the total momentum on uniform and nonuniform points. The local energy and momentum residuals are given in Figs. 7, 8 for uniform points and nonuniform points respectively. It tells us the total energy and momentum are approximated very well whether for uniform or nonuniform points.

Example 3 *(Double solitons).* Consider the collision of double solitons of the NLS equation with the initial condition [52]

$$\eta(x, 0) = \sum_{j=1}^{2} \exp\left(\frac{1}{2} i c_j (x - x_j)\right) \operatorname{sech}(x - x_j). \tag{6.4}$$

In this experiment, we take $c_1 = 1, x_1 = -10, c_2 = -1, x_2 = 10$. The NLS equation with initial condition (6.4) and periodic condition boundary condition $\eta(-50, t) = \eta(50, t)$ is solved till $t = 25$ using the MSQI method. Here the time step is $\tau = 0.001$ and grid number is $N = 1000$. The shape parameter for this example is $c = 0.2h^{1/2}$. The initial phases of two solitary waves are symmetric about origin with equal amplitudes and opposite velocities. The numerical results in Fig. 9 verify this observation vividly. The total energy error and momentum error with uniform centers and nonuniform centers

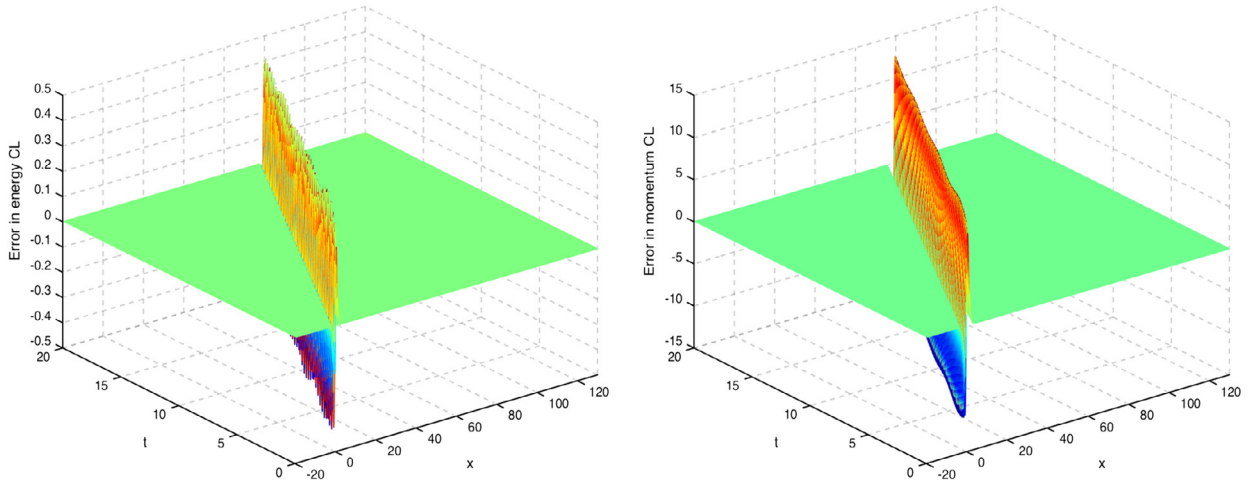

(a) Error in energy CL, nonuniform points (b) Error in momentum CL, nonuniform points

Fig. 8. Numerical errors in local energy and momentum over the time interval $[0, 20]$ on nonuniform points, Example 2.

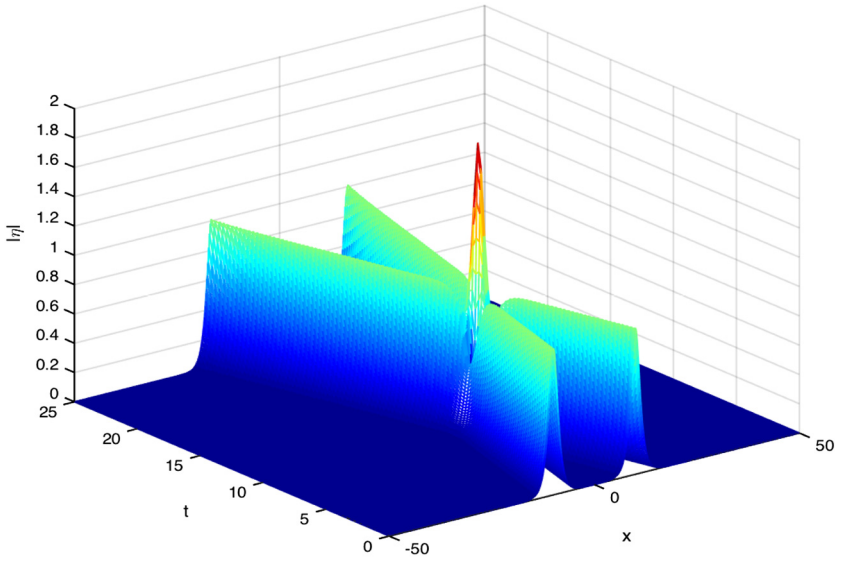

Fig. 9. The wave propagation of two soliton solution with initial condition (6.4) by using MSQI scheme ($\tau = 0.001$, $N = 1000$).

are given in Fig. 10. For comparison, we also present the numerical results by using the second order finite difference method in Fig. 10. Fig. 11 shows the residuals in energy conservation laws and momentum conservation laws for uniform case, while Fig. 12 shows the results for nonuniform case.

Remark 6.1. In the two solitons case, we can observe in Fig. 10 that the error in total momentum is conserved exactly and the error in total energy is bounded whether for uniform or nonuniform centers. Besides, we could see a spike in total energy error which is correspond to the rapid transitions of solution when the double soliton collides [57]. Moreover, from Figs. 11 and 12, we see that the error is focused on the wave propagation path.

6.3. Two-dimensional nonlinear Schrödinger equation

Example 4. Consider the following two-dimensional Schrödinger equation [18,44,46]

$$i\eta_t + \frac{1}{2}(\eta_{xx} + \eta_{yy}) + 2|\eta|^2\eta = 0 \tag{6.5}$$

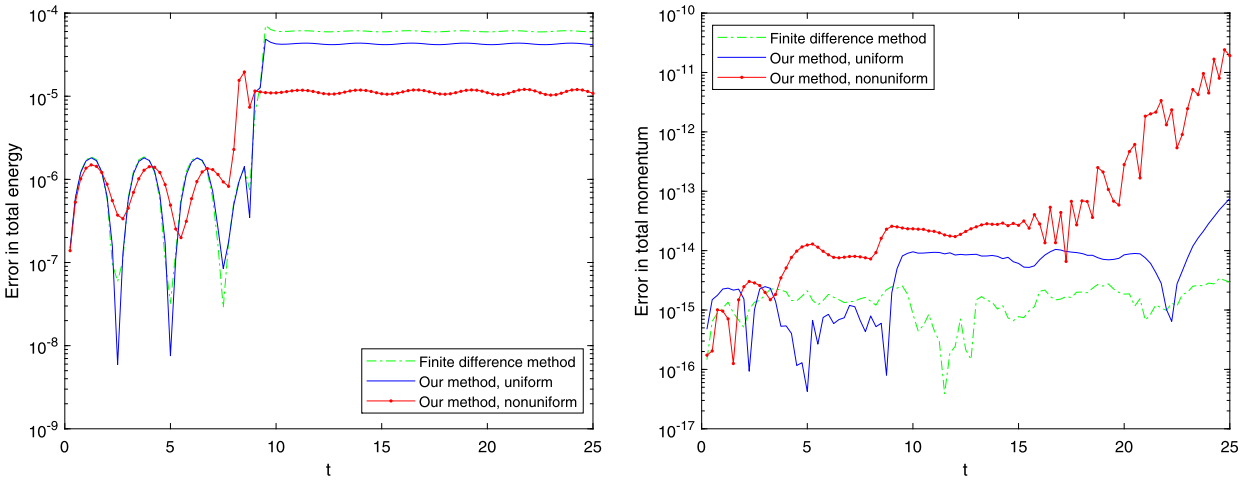

(a) Error in total energy (b) Error in total momentum

Fig. 10. Numerical errors in global energy and momentum over the time interval [0, 25], Example 3.

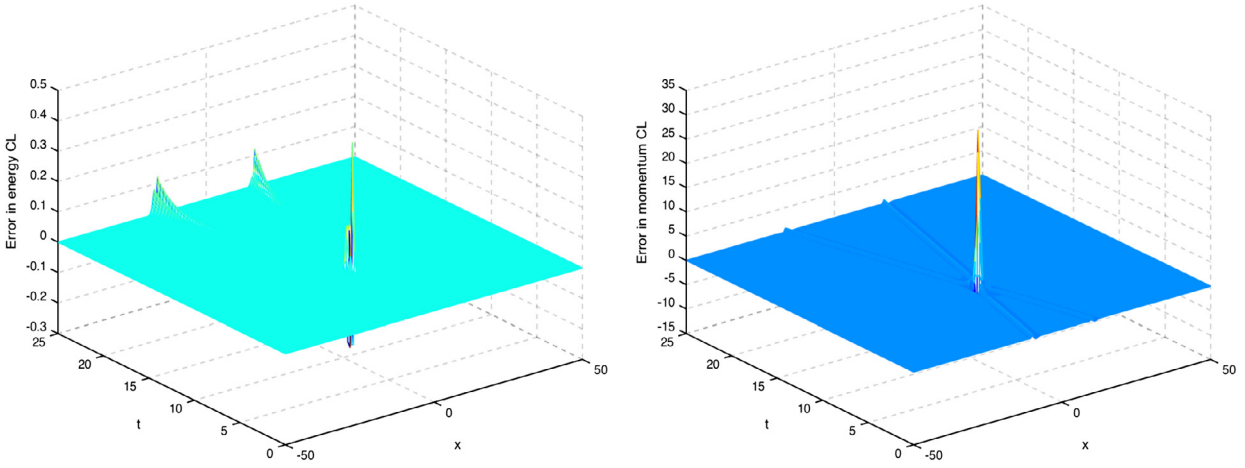

(a) Error in energy CL, uniform points (b) Error in momentum CL, uniform points

Fig. 11. Numerical errors in local energy and momentum over the time interval [0, 25] on uniform points, Example 3.

with homogeneous boundary conditions over $[-10, 10]^2$. The equation has the following analytic solution

$$\eta(x, y, t) = e^{i[2(x+y)-3t]}\text{sech}(x + y - 4t). \tag{6.6}$$

We slove this problem till $t = 4$ by using the full-discrete scheme (5.4) with the Gaussian kernel $\phi_2(x)$ ($\phi_2(x) = \frac{15c^4-10c^2x^2+x^4}{8\sqrt{2\pi}c^5}e^{-\frac{x^2}{2c^2}}$). Fig. 13 depicts the numerical simulations of $|\eta|$ at four different times $t = 0.5, 1, 2, 4$ with time step $\tau = 0.001$, $N = 128$ in each direction and shape parameter $c = 0.4h^{1/2}$. We observe clearly that the soliton wave propagates from the center to the right side. Moreover, Fig. 14 shows the numerical errors in total energy for uniform and nonuniform tensor-product grids. Note that the errors in both cases are bounded and small.

7. Conclusion

Based on quasi-interpolation, we develop a new multi-symplectic method for solving Hamiltonian partial differential equations on multi-symplectic formulation. This is the first attempt for applying quasi-interpolation method to construct multi-symplectic scheme. Using the method of lines, we discretize the multi-symplectic PDE in space with quasi-interpolation method and then obtain the full-discrete multi-symplectic scheme by employing implicit midpoint method in time discretization. The corresponding conservation laws are also verified. Due to the fair properties of quasi-interpolation, our new multi-symplectic quasi-interpolation method is simple, efficient and easy to implement. Besides, our new approach

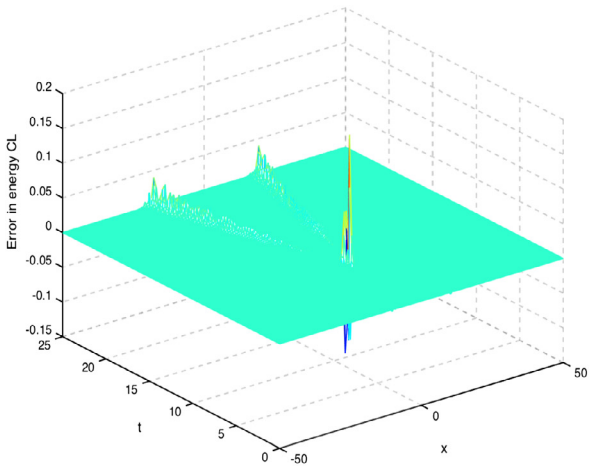

(a) Error in energy CL, nonuniform points

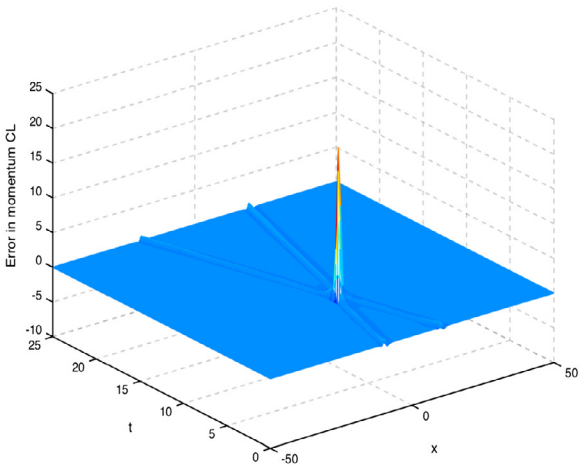

(b) Error in momentum CL, nonuniform points

Fig. 12. Numerical errors in local energy and momentum over the time interval [0, 25] on nonuniform points, Example 3.

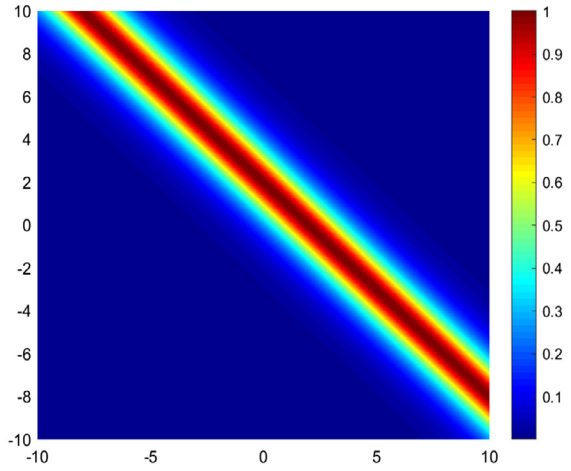

(a) t=0.5

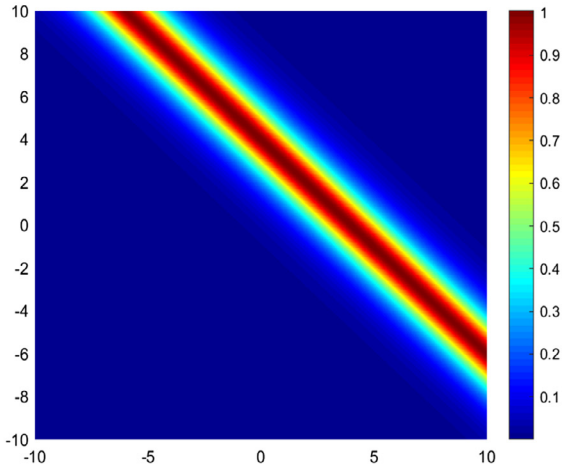

(b) t=1

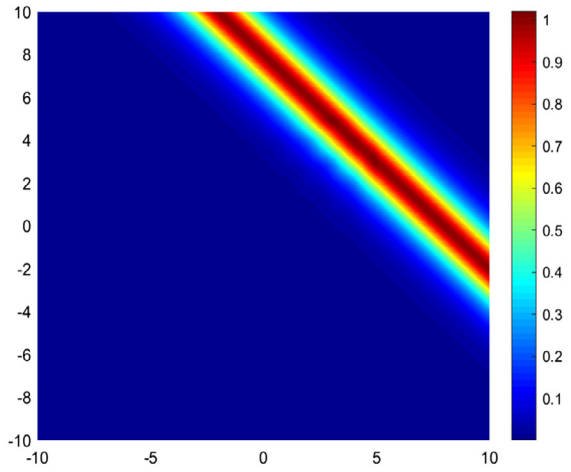

(c) t=2

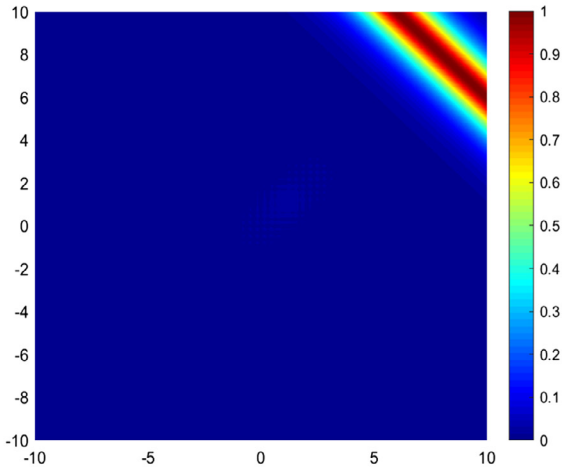

(d) t=4

Fig. 13. Images $|\eta|$ for the numerical solution of 2D Schrödinger equation (6.5) at times $t = 0.5, 1, 2, 4$, Example 4.

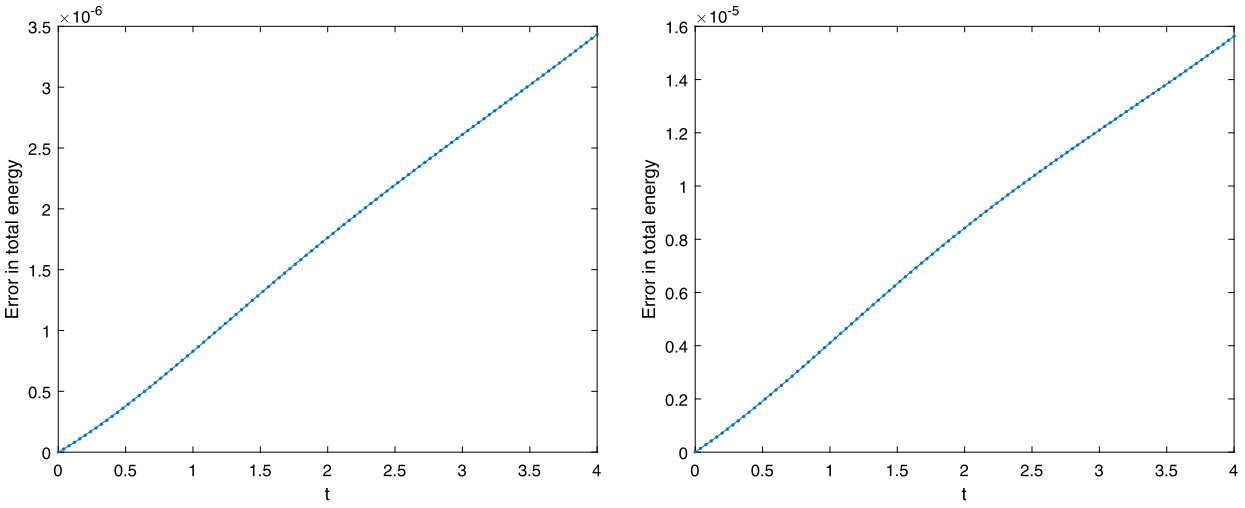

(a) Error in total energy, uniform (b) Error in total energy, nonuniform

Fig. 14. Numerical errors in total energy over the time interval [0, 4] of the 2D Schrödinger equation (6.5), Example 4.

is also valid on nonuniform grids which is superior to other traditional methods. It could be employed in developing adaptive conservative methods which will be pursued in our future work.

Acknowledgements

We thank the anonymous reviewers for their valuable comments. This work is supported by National Natural Science Foundation of China (11631015) and Hong Kong Scholars Program (2018046).

References

[1] R.K. Beatson, M.J.D. Powell, Univariate multiquadric approximation: quasi-interpolation to scattered data, Constr. Approx. 8 (1992) 275–288.
[2] A.G. Bratsos, A fourth order numerical scheme for the one-dimensional sine-Gordon equation, Int. J. Comput. Math. 85 (2008) 1083–1095.
[3] T.J. Bridges, Multi-symplectic structures and wave propagation, Proc. R. Soc. Lond. Ser. A 455 (1997) 147–190.
[4] T.J. Bridges, S. Reich, Multi-symplectic integrators: numerical schemes for Hamiltonian PDEs that conserve symplecticity, Phys. Lett. A 284 (2001) 184–193.
[5] T.J. Bridges, S. Reich, Multi-symplectic spectral discretizations for the Zakharov-Kuznetsov and shallow water equations, Phys. D 152 (2001) 491–504.
[6] M. Buhmann, Convergence of univariate quasi-interpolation using Multiquadrics, IMA J. Numer. Anal. 8 (1988) 365–383.
[7] M. Buhmann, N. Dyn, D. Levin, On quasi-interpolation by radial basis function with scattered data, Constr. Approx. 11 (1995) 239–254.
[8] M.D. Buhmann, Radial Basis Functions: Theory and Implementations, Cambridge University Press, 2003.
[9] B. Cano, J.M. Sanz-Serna, Error growth in the numerical integration of periodic orbits, with application to Hamiltonian and reversible systems, SIAM J. Numer. Anal. 34 (4) (1997) 1391–1417.
[10] J.B. Chen, M.Z. Qin, Multi-symplectic Fourier pseudospectral method for the nonlinear Schrödinger equation, Electron. Trans. Numer. Anal. 12 (2001) 193–204.
[11] R.H. Chen, Z.M. Wu, Applying multiquadric quasi-interpolation to solve Burgers' equation, Appl. Math. Comput. 172 (1) (2006) 472–484.
[12] D. Cohen, B. Owren, X. Raynaud, Multi-symplectic integration of the Camassa-Holm equation, J. Comput. Phys. 227 (11) (2008) 5492–5512.
[13] C. de Boor, G.J. Fix, Spline approximation by quasi-interpolants, J. Approx. Theory 8 (1973) 19–45.
[14] J. de Frutos, J.M. Sanz-Serna, Accuracy and conservation properties in numerical integration: the case of the Korteweg-de Vries equation, Numer. Math. 75 (1997) 421–445.
[15] M. Dehghan, M. Abbaszadeh, The use of proper orthogonal decomposition (POD) meshless RBF-FD technique to simulate the shallow water equations, J. Comput. Phys. 351 (2017) 478–510.
[16] M. Dehghan, M. Abbaszadeh, Solution of multi-dimensional Klein-Gordon-Zakharov and Schrödinger/Gross-Pitaevskii equations via local Radial Basis Functions-Differential Quadrature (RBF-DQ) technique on non-rectangular computational domains, Eng. Anal. Bound. Elem. 92 (2018) 156–170.
[17] M. Dehghan, M. Abbaszadeh, A. Mohebbi, The numerical solution of the two-dimensional sinh-Gordon equation via three meshless methods, Eng. Anal. Bound. Elem. 51 (2015) 220–235.
[18] M. Dehghan, V. Mohammadi, A numerical scheme based on radial basis function finite difference (RBF-FD) technique for solving the high-dimensional nonlinear Schrödinger equations using an explicit time discretization: Runge-Kutta method, Comput. Phys. Commun. 217 (2017) 23–34.
[19] M. Dehghan, A. Shokri, A numerical method for two-dimensional Schrödinger equation using collocation and radial basis functions, Comput. Math. Appl. 54 (2007) 136–146.
[20] M. Dehghan, A. Shokri, A numerical method for solution of the two-dimensional sine-Gordon equation using the radial basis functions, Math. Comput. Simul. 79 (3) (2008) 700–715.
[21] M. Dehghan, A. Shokri, Numerical solution of the nonlinear Klein-Gordon equation using radial basis functions, J. Comput. Appl. Math. 230 (2) (2009) 400–410.
[22] G. Fix, G. Strang, A Fourier analysis of the finite element method, in: Constructive Aspects of Functional Analysis, CIME I, vol. 1, 1970, pp. 793–840.
[23] D. Furihata, Finite-difference schemes for nonlinear wave equation that inherit energy conservation property, J. Comput. Appl. Math. 134 (1–2) (2001) 37–57.

[24] W.W. Gao, Z.M. Wu, Approximation orders and shape preserving properties of the multiquadric trigonometric B-spline quasi-interpolant, Comput. Math. Appl. 69 (7) (2015) 696–707.
[25] W.W. Gao, Z.M. Wu, Constructing radial kernels with higher-order generalized Strang-Fix conditions, Adv. Comput. Math. 43 (6) (2017) 1355–1375.
[26] Y.Z. Gong, Q. Wang, Y.S. Wang, J.X. Cai, A conservative Fourier pseudo-spectral method for the nonlinear Schrödinger equation, J. Comput. Phys. 328 (2017) 354–370.
[27] Y.C. Hon, Z.M. Wu, A quasi-interpolation method for solving stiff ordinary differential equations, Int. J. Numer. Methods Eng. 48 (8) (2000) 1187–1197.
[28] J.L. Hong, C. Li, Multi-symplectic Runge-Kutta methods for nonlinear Dirac equations, J. Comput. Phys. 11 (2) (2006) 448–472.
[29] J.L. Hong, H.Y. Liu, G. Sun, The multi-symplecticity of partitioned Runge-Kutta methods for Hamiltonian PDEs, Math. Comput. 75 (253) (2006) 167–181.
[30] L.H. Kong, J.J. Zhang, Y. Cao, Y.L. Duan, H. Huang, Semi-explicit symplectic partitioned Runge-Kutta Fourier pseudo-spectral scheme for Klein-Gordon-Schrödinger equations, Comput. Phys. Commun. 181 (8) (2010) 1369–1377.
[31] H. Liu, K. Zhang, Multi-symplectic Runge-Kutta-type methods for Hamiltonian wave equations, IMA J. Numer. Anal. 26 (2) (2006) 252–271.
[32] H.L. Liu, N.Y. Yi, A Hamiltonian preserving discontinuous Galerkin method for the generalized Korteweg-de Vries equation, J. Comput. Phys. 321 (2016) 776–796.
[33] L.M. Ma, Z.M. Wu, Approximation to the k-th derivatives by multiquadric quasi-interpolation method, J. Comput. Appl. Math. 231 (2) (2009) 925–932.
[34] L.M. Ma, Z.M. Wu, Stability of multiquadric quasi-interpolation to approximate high order derivatives, Sci. China Math. 53 (4) (2010) 985–992.
[35] J.E. Marsden, G.P. Patrick, S. Shkoller, Multisymplectic geometry, variational integrators, and nonlinear PDEs, Commun. Math. Phys. 199 (1999) 351–395.
[36] B. Moore, S. Reich, Backward error analysis for multi-symplectic integration methods, Numer. Math. 95 (2003) 625–652.
[37] M. Oliver, M. West, C. Wulff, Approximate momentum conservation for spatial semidiscretizations of semilinear wave equations, Numer. Math. 97 (3) (2004) 493–535.
[38] C. Rabut, An introduction to Schoenberg's approximation, Comput. Math. Appl. 24 (1991) 139–175.
[39] S. Reich, Multi-symplectic Runge-Kutta collocation methods for Hamiltonian wave equations, J. Comput. Phys. 157 (2000) 473–499.
[40] R. Schaback, The missing Wendland functions, Adv. Comput. Math. 34 (1) (2011) 67–81.
[41] J.Q. Sun, M.Z. Qin, Multi-symplectic methods for the coupled 1D nonlinear Schrödinger system, Comput. Phys. Commun. 155 (2003) 221–235.
[42] Z.J. Sun, A meshless symplectic method for two-dimensional nonlinear Schrödinger equations based on radial basis function approximation, Eng. Anal. Bound. Elem. 104 (2019) 1–7.
[43] Z.J. Sun, Z.M. Wu, Meshless conservative scheme for nonlinear Hamiltonian partial differential equations, J. Sci. Comput. 76 (2018) 1168–1187.
[44] A. Taleei, M. Dehghan, Time-splitting pseudo-spectral domain decomposition method for the soliton solutions of the one- and multi-dimensional nonlinear Schrödinger equations, Comput. Phys. Commun. 185 (6) (2014) 1515–1528.
[45] W.S. Tang, Y.J. Sun, W.J. Cai, Discontinuous Galerkin methods for Hamiltonian ODEs and PDEs, J. Comput. Phys. 330 (2017) 340–364.
[46] H.Q. Wang, An efficient Chebyshev-Tau spectral method for Ginzburg-Landau-Schrödinger equations, Comput. Phys. Commun. 181 (2) (2010) 325–340.
[47] Z.M. Wu, Dynamically knots setting in meshless method for solving time dependent propagations equation, Comput. Methods Appl. Mech. Eng. 193 (12–14) (2004) 1221–1229.
[48] Z.M. Wu, J.P. Liu, Generalized Strang-Fix condition for scattered data quasi-interpolation, Adv. Comput. Math. 23 (2005) 201–214.
[49] Z.M. Wu, S.L. Zhang, Conservative multiquadric quasi-interpolation method for Hamiltonian wave equations, Eng. Anal. Bound. Elem. 37 (7–8) (2013) 1052–1058.
[50] Z.M. Wu, S.L. Zhang, A meshless symplectic algorithm for multi-variate Hamiltonian PDEs with radial basis approximation, Eng. Anal. Bound. Elem. 50 (2015) 258–264.
[51] Y. Xu, C.W. Shu, Local discontinuous Galerkin methods for three classes of nonlinear wave equations, J. Comput. Math. (2004) 250–274.
[52] Y. Xu, C.W. Shu, Local discontinuous Galerkin methods for nonlinear Schrödinger equations, J. Comput. Phys. 205 (2005) 72–97.
[53] N.Y. Yi, Y.Q. Huang, H.L. Liu, A direct discontinuous Galerkin method for the generalized Korteweg-de Vries equation: energy conservation and boundary effect, J. Comput. Phys. 242 (2013) 351–366.
[54] L. Zhen, Y.Q. Bai, K. Wu, Symplectic and multi-symplectic schemes with finite element methods, Phys. Lett. A 314 (2003) 443–455.
[55] C.G. Zhu, R.H. Wang, Numerical solution of Burgers' equation by cubic B-spline quasi-interpolation, Appl. Math. Comput. 208 (1) (2009) 260–272.
[56] H.J. Zhu, Y.M. Chen, S.H. Song, H.Y. Hu, Symplectic and multi-symplectic wavelet collocation methods for two-dimensional Schrödinger equations, Appl. Numer. Math. 61 (2011) 308–321.
[57] H.J. Zhu, S.H. Song, Y.F. Tang, Multi-symplectic wavelet collocation methods for the nonlinear Schrödinger equation and the Camassa-Holm equation, Comput. Phys. Commun. 182 (2011) 616–627.
[58] H.J. Zhu, L.Y. Tang, S.H. Song, Y.F. Tang, D.S. Wang, Symplectic wavelet collocation method for Hamiltonian wave equations, J. Comput. Phys. 229 (2010) 2550–2572.